 DOI 10.1515/aot-2012-0048 — Adv. Opt. Techn. 2012; 1(6): 427–439

Review Article

Ralf D. Geckeler*, Oliver Kranz, Andreas Just and Michael Krause

A novel approach for extending autocollimator calibration from plane to spatial angles

Abstract: Autocollimators are versatile devices for the contactless measurement of the tilt angles of reflecting surfaces. In their practical application, e.g., in deflectometric profilometers for the precision form measurement of optical surfaces, the autocollimator beam is deflected in two orthogonal angular directions simultaneously. The concurrent engagement of both measuring axes results in errors in their angle response due to the crosstalk between them, which need to be calibrated. In this contribution, the capabilities of autocollimator calibration at the Physikalisch-Technische Bundesanstalt (PTB) are presented. The measurement of spatial angles is discussed in detail with a focus on achieving traceability of this measurand and reaching lowest uncertainties. A novel concept is introduced, which makes use of an innovative Cartesian arrangement of three autocollimators (two reference autocollimators and the autocollimator to be calibrated) facing a reflector cube. Each of the two reference autocollimators, which are used for the precise measurement of the cube's angular orientation, is primarily sensitive to rotations of the cube around one of the two relevant axes and can, thus, be calibrated and traced back to PTB's national primary standard for the plane angle in a conventional manner. In this way, the measurement of spatial angles is effectively divided into two separate measurements of plane angles. The mechanical realisation of the setup at PTB is described.

Keywords: angle metrology; autocollimator; calibration; crosstalk error; spatial angle.

***Corresponding author: Ralf D. Geckeler,** Physikalisch-Technische Bundesanstalt, Bundesallee 100, D-38116 Braunschweig, Deutschland, e-mail: ralf.geckeler@ptb.de
Oliver Kranz, Andreas Just and Michael Krause: Physikalisch-Technische Bundesanstalt, Bundesallee 100, D-38116 Braunschweig, Deutschland

1 Introduction

During the last decade, important advances in the precision form measurement of optical surfaces have been achieved by a new generation of angle-based (deflectometric) surface profilometers (e.g., [1–7]). For the contactless measurement of the local surface slope (tilt angle), commercial high-resolution autocollimators are used, which are capable of providing precise and traceable angle metrology for this purpose. When compared to classical interferometry, deflectometric profilometry is of advantage for measuring optical surfaces that are demanding due to their extent, their high dynamic topography range and gradients, and when the need for absolute topography measurement arises (i.e., without recourse to external standards, such as calibrated reference surfaces).

Because of these advantages, deflectometric profilometry has turned out to be especially capable of accurately measuring beam-shaping optical surfaces for applications in the next generation synchrotron beamlines and free electron lasers (FEL). Owing to their large size (up to 1.5 m), aspherical, rotationally asymmetric shape and extremely stringent demands on their form accuracy (2 nm peak-to-valley in form, 50 nrad root-mean-squared in slope [8, 9]), they pose equally stringent demands on the characterisation and calibration of the autocollimators, which are used for their measurement. Autocollimator calibration under well-defined, stable and reproducible measurement conditions is central to making full use of their potential by correcting their angle measurement errors and, therefore, is essential for approaching fundamental metrological limits in deflectometric form measurement. For a comprehensive overview of their use in deflectometric profilometers and the specific challenges associated with this application (see [10–12]).

Two challenges, which are of special importance to the measurement of synchrotron and FEL optics, are the extension of traceable angle calibration from the plane angle to spatial angles and the characterisation of the effects of the optical path length changes of the autocollimator beam on its angle measurement (the path length variability of the autocollimator beam is a result of the scanning of extended

optical surfaces). Beam-shaping optics in synchrotrons and FEL often feature rotationally asymmetric, aspherical surfaces, which, when their form is measured in deflectometric profilometers, may deflect the surface-probing autocollimator beam perpendicular to the main profiling direction. Therefore, in the practical application of an autocollimator, both of its measurement axes are engaged simultaneously, i.e., the autocollimator beam is reflected in two orthogonal angular directions by the surface. For such an advanced autocollimator calibration, innovative strategies and novel equipment needed to be developed.

In this paper, we focus on the challenges to traceable angle metrology with autocollimators, which are posed by spatial angles. In Section 2, we provide a report on the current status of traceable autocollimator calibration with high angular resolution and lowest uncertainty at PTB by means of its ultraprecision primary angle standard WMT 220. We also provide information on factors influencing the angle response of autocollimators. In Section 3, we discuss traceability issues of plane and spatial angles in detail, including a discussion on the SI definition of the derived angle unit 'radian' and the alternative realisations by circle division methods. In Section 4, a novel concept for the realisation of spatial angle calibration is presented, which has been developed at PTB and which makes use of an innovative Cartesian arrangement of three autocollimators facing a reflector cube. In Section 5, we analyse the geometrical aspects of spatial angle measurement, in general, with a focus on the derivation of analytical expressions for the angle measurements by the autocollimators in our Cartesian configuration. In Section 6, we briefly discuss alignment errors, their influence on spatial angle measurement, their evaluation and their compensation. In Section 7, the technical realisation of our spatial angle autocollimator calibrator (SAAC) is described in detail, and information on the status of the setup is provided.

2 Current status of autocollimator calibration at PTB

The WMT 220 angle comparator (Figure 1) of PTB serves as the primary national standard for the plane angle in Germany and is used for the most accurate calibrations of angle artefacts or angle-measuring instruments. It was custom-made by Dr. Johannes Heidenhain GmbH, Traunreut, Germany. The WMT 220 consists of a precision air-bearing rotary table equipped with a radial phase grating (400 mm in diameter, 2^{17} grating lines) and an interferential measuring system with eight photoelectric scanning heads, which are distributed at regular 45° intervals. Additionally, eight auxiliary scanning heads are arranged in pairs – diametrically opposed to each other – to form angle intervals of $360°/2^n$ with $1 \geq n \geq 7$, with the smallest being 2.81° (see [13] for further technical details).

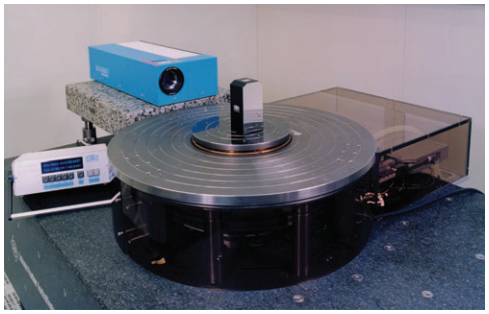

Figure 1 The WMT 220 angle comparator of PTB is the primary national standard of plane angle in Germany. Its calibration uncertainty is u=0.001 arcsec (5 nrad). It is installed in a clean-room facility and, thus, operates under favourable environmental conditions, such as a highly stable ambient temperature (ΔT<0.05 K). A measurement setup for the calibration of an electronic autocollimator is shown.

The systematic graduation errors of the grating can be determined by two independent methods: classical cross-calibration (against a built-in or external secondary angle encoder [14–17]) and self-calibration. At PTB, extensive research on the fast and precise *in situ* self-calibration of angle encoders has been carried out [18, 19]. This method relies on a suitable geometric arrangement of multiple reading heads, which read out the radial grating of the angle encoder at different angular positions. The self-calibration analysis is performed most naturally in the frequency domain, as all reading heads are assumed to measure the same – albeit phase-shifted – graduation errors of the grating. Using the Fourier shift theorem to account for the phase shift, the graduation errors can be reconstructed by analysing the measurement differences between pairs of reading heads by the use of variance-optimal weights to achieve a more uniform error propagation (see [18] for further details). Self-calibration offers a number of advantages, foremost that it is independent of auxiliary devices (such as, e.g., a secondary angle encoder or a polygon). As part of the family of circle division methods, it utilises the full circle as a natural, error-free angular standard, which provides independence from external reference standards (see Section 2). Furthermore, in contrast to cross-calibration, self-calibration is fast and, therefore, ideally suited for industrial applications.

The standard uncertainty of the calibration of the WMT 220 is of the order of u=0.001 arcsec (5 nrad) and has been verified by various internal comparisons (of

cross- and self-calibrations) and comparisons with encoders of external partners, which all demonstrate consistency at the level of several nrad rms (see, e.g., [20]).

By comparison with the WMT 220, autocollimators can be calibrated down to a standard uncertainty of approximately u=0.004 arcsec (19 nrad) [11, 12, 21]. Figure 2 shows an example of a high-resolution autocollimator calibration at a small aperture (2.5 mm), which is typical for autocollimator applications in deflectometric profilometers. The uncertainty budget for an autocollimator calibration is dominated by contributions by the autocollimator itself, which depend on the calibration parameters influencing its angle response. Therefore, calibrations at PTB are usually performed flexibly according to user specifications of these influencing parameters, such as the reflectivity of the surface under test, the aperture stop's diameter, shape, as well as its position both along the autocollimator's optical axis and perpendicular to it [12], and the optical path length of the autocollimator beam [11]. First, the experimental results on the influences of the surface under test curvature have also been obtained [10] and are currently investigated by ray tracing modelling of autocollimators.

Autocollimator calibrations depend sensitively on the calibration parameters, and they are valid for a specific parameter set only. Most deflectometric profilometers use a movable pentaprism to scan the surface under test, which induces large (in the range of 1–2 m) and unavoidable changes in the optical path length of the autocollimator beam, which in turn cause the returning beam to follow different geometric paths through the autocollimator's optics. Owing to the interaction with aberrations and alignment errors of the autocollimator's optical components, path-dependent angle measurement deviations are induced (see [10, 11] for further details). At PTB, we are currently able to accurately calibrate autocollimators at discrete distances (250–550 mm) from the reflecting surface only. Therefore, the capability of large (up to 1.5 m) and automatic changes in the path length between the autocollimator and the reflector cube has been implemented in our new calibration device (see Section 7). We are also collaborating – together with the Helmholtz-Zentrum Berlin (HZB), Germany – with the Advanced Light Source (ALS), Berkeley, USA, in the development of the Universal Test Mirror (UTM) to address this crucial issue [22].

Recently, advanced error-separating shearing techniques for the cross-calibration of angle measuring devices (which have originally been developed for application to shearing interferometry [23–25]) have been adapted to autocollimator calibration and tested at PTB. Autocollimator calibration usually relies on the comparison with a calibrated angle reference standard. Shearing techniques, by applying defined angular offsets between both systems, offer a unique opportunity to separate the errors of the autocollimator and of the second system and, therefore, to calibrate both systems without recourse to any external standard; instead, they are self-reliant. The results of the first experimental tests at PTB with an autocollimator and our primary standard WMT 220 were promising, with an error separation at a level of approximately 0.001 arcsec (5 nrad) rms.

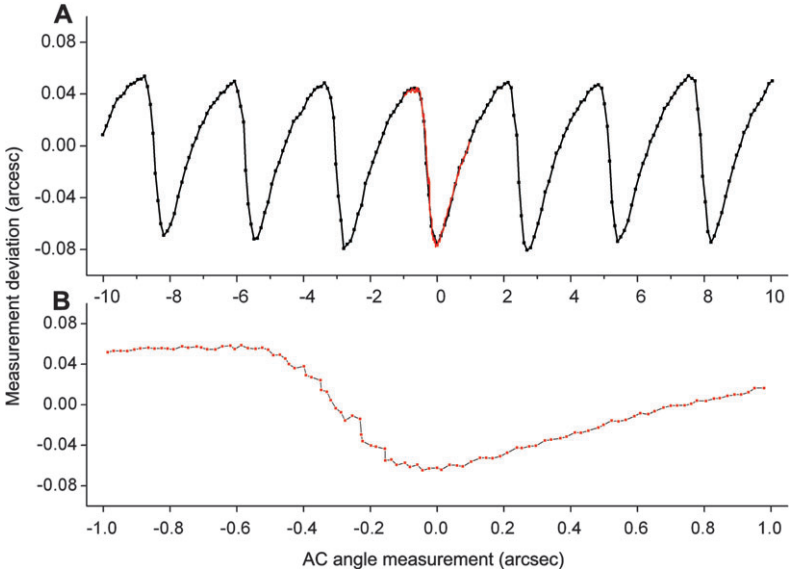

Figure 2 High-resolution calibration data of a commercial electronic autocollimator over a limited measurement range of 10 and 1 arcsec. At a small aperture (2.5 mm), angle deviations on a scale of 2.8 arcsec are present, which corresponds to the pixel size of the autocollimator's CCD detector. (A) Calibration range of 10 arcsec, sampling 0.1 arcsec. (B) Calibration range of 1 arcsec, sampling 0.02 arcsec.

3 Extension of autocollimator calibration to spatial angles

In the practical application of autocollimators, e.g., in deflectometric profilometers, both of the autocollimator's measuring axes are engaged simultaneously, i.e., the autocollimator beam is deflected in two orthogonal angular directions by the surface under test. The same holds true for most applications in precision engineering, e.g., the measurement of machine geometries (straightness, flatness and parallelism), where both autocollimator axes are also utilised concurrently. The simultaneous engagement of both measuring axes results in additional errors in their angle response due to the crosstalk between the axes, i.e., the angle measurements of the axes are interdependent to a certain degree. This crosstalk is caused by, e.g., alignment errors of the autocollimator's internal optomechanical components (which, effectively, result in the non-orthogonality of the measuring axes), optical aberrations of its optical components and geometrical imperfections of the reticles, which are imaged onto the autocollimator's detector(s). Additionally, spatial angles may be calculated incorrectly by the autocollimator's software when both axes are incorrectly treated, as if their measurements were totally independent of each other (see Section 5).

The crosstalk between the measuring axes is a general problem of spatial angle measurement by all methods, including, e.g., angle interferometers. Therefore, to provide full traceability of spatial angles to primary angle standards (which is currently available for the plane angle only) is a nontrivial problem. Here, 'traceability of measurands' is a metrological concept with the aim to provide a stringent control of measurements performed by a device. It is the 'property of the result of a measurement or the value of a standard, whereby it can be related to stated references, usually national or international standards, through an unbroken chain of comparisons all having stated uncertainties' ([26], see also [27]).

According to the Système International d'Unités [28], the unit 'radian' of the plane angle is formally derived from the SI base unit 'metre' as the ratio of the length of the arc of a circle's segment to its radius according to 1 rad=1 m/1 m. Such angle realisations by means of dimensional quantities are provided, e.g., by sine bars based on length interferometers or displacement sensors. However, this angle realisation poses two problems: First, that light does not follow an arc, but a straight line, and second, that it is exceedingly difficult or impossible to measure the effective radius, e.g., the distance between the centres-of-light of the interferometer beams or that between mechanical displacement sensors. Let us ignore the latter caveat and assume the use of straight lines of precisely known length. Attempts to define an angle using two straight lines necessitate additional knowledge on the angle between the lines (usually they are arranged perpendicular to each other). Therefore, they are not adequate for providing a consistent angle realisation, based on length measurement, which is suitable for a primary standard. Only three straight lines define an angle in an unequivocal manner, which allows deriving the unit 'radian' of the plane angle consistently from the SI base unit 'metre'.

However, alternative methods are available, which circumvent these problems: the circle subdivision methods for circular angle encoders. The techniques are generally based on the subdivision of the full circle and make use of circle closure, expressing the fact that the sum of the angles of a divided full circle in a plane equals 2π. The full circle, therefore, represents a natural and error-free angular standard of 2π rad, and its graduation has always been a fundamental method of representing the angular scale. To this purpose, different cross- and self-calibration methods can be applied [14–19].

In the practical implementation of circle division methods, angle encoders with circular scales are used so that only plane angles can be realised by these methods, not spatial angles (see Section 2). In the following section, we demonstrate our concept of separating the measurement of the spatial angle of a reflector cube into separate measurements of plane angles by a Cartesian arrangement of angle measuring devices. Note that the use of spherical gratings would allow extending the circle division method to spatial angles by using the full closure across the sphere. However, no technical realisations of such encoders exist. In an analogous way, when stellar astrometry is performed across the entire sky, the closure condition can be applied to reduce errors in angle measurements.

4 Concept of the spatial angle autocollimator calibrator

To extend the traceable autocollimator calibration to spatial angles, innovative strategies and novel equipment needed to be developed. At PTB, work had been done on a two-axis piezoelectric device for autocollimator calibration [29]. However, due to its limited stability, the achieved level of uncertainty was not sufficient to satisfy the stringent demands on autocollimator calibrations posed by deflectometric profilometers (see Section 1). Therefore, we

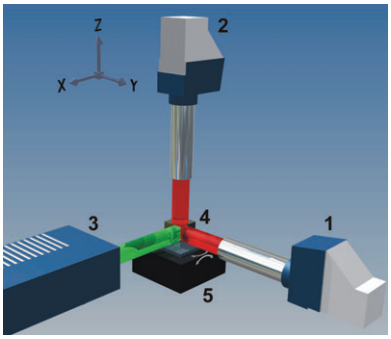

Figure 3 Cartesian arrangement of three autocollimators facing a reflector cube for spatial angle calibration. Its main components are two reference autocollimators, a horizontal (1) and a vertical one (2), the autocollimator to be calibrated (3), and a reflector cube (4). The cube's angular orientation with respect to the y and z axes (the pitch and yaw angles as seen from the autocollimator to be calibrated) are manipulated by a two-axis tilting system (5).

developed a novel system for the calibration of autocollimators, which makes use of an innovative Cartesian configuration of three autocollimators (two reference autocollimators and the autocollimator to be calibrated) in space, which are facing a reflector cube, the SAAC (see Figure 3).

To circumvent problems with the traceability of spatial angle measurement (see Section 3 for details), each reference autocollimator is sensitive primarily to rotations of the cube around one of the two relevant axes (the y and z axes, with corresponding yaw and pitch angles, respectively, as seen from the autocollimator to be calibrated). In this way, the measurement of the angular orientation of the reflector cube is effectively divided into two separate measurements of plane angles by the reference autocollimators. Therefore, each reference autocollimator can be calibrated in a conventional manner, i.e., its measurements can be traced back to our national primary standard WMT 220 for the plane angle. In contrast, the autocollimator to be calibrated is sensitive to rotations of the cube around both relevant axes. In Section 5, we provide more information on the angle response of each autocollimator by deriving analytical expressions for the angle measurements by the autocollimators in our Cartesian configuration. In Section 7, the SAAC's technical realisation is described in detail.

5 Angle responses of the SAAC's autocollimators

Autocollimators perform contact-free measurements of the angle of a reflecting surface relative to the optical axis of the device. Thereby, a light beam coming from the autocollimator along its optical axis is reflected by the surface, and the deflection angle of the returning beam is measured. In this section and the appendix, the deflection angles of the autocollimator beams are derived for the Cartesian autocollimator configuration of the SAAC for an arbitrary angular orientation of the reflector cube in space.

Figure 4 shows the definition of the polar coordinates λ and δ of the normal vector $\hat{n}$ of the reflector cube's frontal surface (see also the geometrical setup of the SAAC, Figure 3). The coordinate system is defined by the autocollimator's optical axis and its horizontal and vertical measuring axes (they correspond to the x, y and z axes, respectively). Note that, due to the specific stacking of the different rotational axes in the mechanical realisation of our device, these polar coordinates correspond directly to the angles, which are measured by the axes' angle encoders (as the cube is first rotated around the z axis and then rotated around the y′ axis, which results from the y axis by the first rotation).

In the Appendix, the polar coordinates $\tilde{\lambda}$ and $\tilde{\delta}$ of the reflected beam of the autocollimator to be calibrated are derived. For a better intuitive understanding of the results, we consider their approximations up to the third order (which are applicable for small angles $\alpha << \pi$):

$$\tilde{\delta} \approx 2\delta - \lambda^2\delta \quad \text{and} \tag{1}$$

$$\tilde{\lambda} \approx 2\lambda + 2\lambda\delta^2. \tag{2}$$

Therefore, in the case of an arbitrary angular orientation of a reflecting surface in space, each component of the polar coordinates of the reflected autocollimator beam is not exactly equal to twice the corresponding component of the surface normal. Instead, there is an angular crosstalk between the components, which is of purely

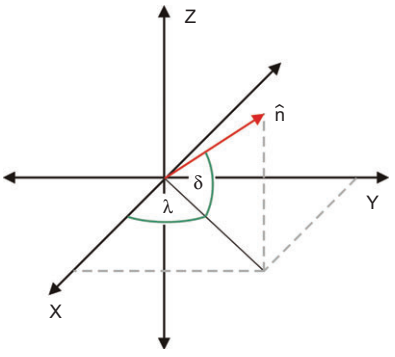

Figure 4 Inscribed x-y-z coordinate system and polar coordinates λ and δ of the normal vector $\hat{n}$ of the reflector cube's frontal surface (see also Figure 3).

geometrical origin and not connected to the crosstalk due to imperfections of the autocollimator's optomechanical components and their alignment. Figure 5A shows the deviation $\tilde{\lambda}$-2λ of the angle $\tilde{\lambda}$ of the reflected beam from twice the surface inclination angle λ for values of λ and δ in the range ±2000 arcsec. Figure 5B shows the respective deviation $\tilde{\delta}$-2δ. Usually, the autocollimator software does not account for this geometrical effect, but treats both axes incorrectly as if their measurements were totally independent of each other.

In the case of the horizontal reference autocollimator, its optical axis and its horizontal and vertical measuring axes correspond to the y, (-x) and z axes, respectively. For a better intuitive understanding of the results, we define a new polar coordinate system with angles $\tilde{\lambda}'$ and $\tilde{\delta}'$, which are connected to the horizontal reference autocollimator, i.e., the new polar coordinates represent a local view of the beam deflection by this autocollimator (i.e., the x-y-z coordinates from Figure 4 are replaced by the y-(-x)-z coordinates). In the Appendix, the polar coordinates $\tilde{\lambda}'$ and $\tilde{\delta}'$ of the reflected beam of the horizontal reference autocollimator are derived as

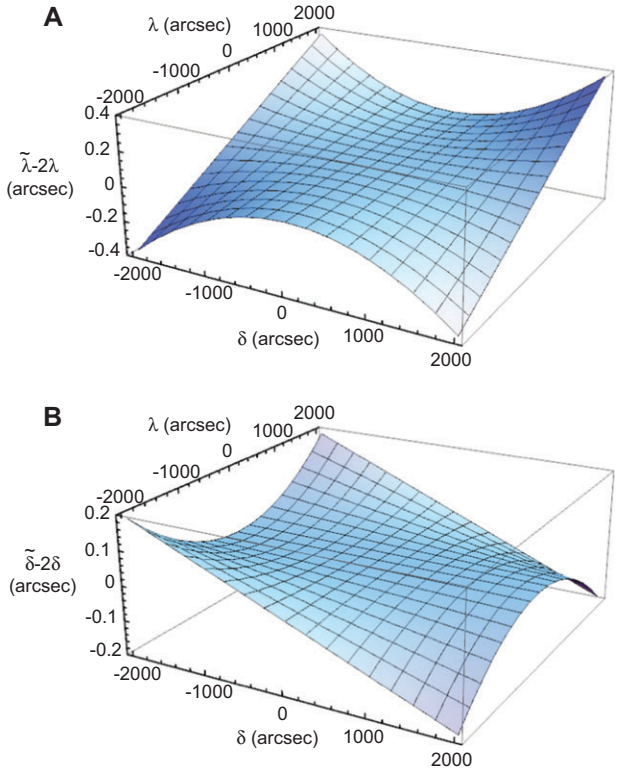

Figure 5 For a reflecting surface with an arbitrary angular orientation, each component of the polar coordinate of the reflected beam is not exactly equal to twice the corresponding component of the surface normal. (A) Angle difference $\tilde{\lambda}$-2λ for values of λ and δ in the range ±2000 arcsec, (B) corresponding deviation $\tilde{\delta}$-2δ.

$$\tilde{\delta}' \equiv 0 \quad \text{and} \tag{3}$$

$$\tilde{\lambda}' \equiv 2\lambda. \tag{4}$$

These relations are exact; they are not approximations. In the same way, the angle of the reflected measuring beam of the vertical reference autocollimator can be derived. Its optical axis and its horizontal and vertical measuring axes correspond to the z, y and (-x) axes, respectively. In the Appendix, the polar coordinates $\tilde{\lambda}''$ and $\tilde{\delta}''$ of the reflected beam of the vertical reference autocollimator are derived (we use a polar coordinate system that represents a local view of the beam deflection by this autocollimator again). Their approximations up to the third order are given by:

$$\tilde{\delta}'' = \tilde{\delta} \approx 2\delta - \lambda^2\delta \quad \text{and} \tag{5}$$

$$\tilde{\lambda}'' = -2\lambda\delta. \tag{6}$$

Figure 6 shows the polar coordinates of the deflected autocollimator beams in the SAAC setup [as detected locally by each autocollimator; see equations (1)–(6)] when the reflector cube scans a regular grid of spatial angles for the autocollimator to be calibrated. As the readout of an autocollimator is not defined as the deflection angle of the returning beam itself, but as the equivalent tilting angle of a surface resulting in the same deflection (i.e., 1/2 of the deflection angle), the angles have been divided by a factor of 2. In the case of the horizontal reference autocollimator, only its main measurement axis is engaged (the horizontal measuring axis in Figure 6B). In the case of the vertical reference autocollimator, however, not only is its main measurement axis engaged (the vertical axis in Figure 6C) but also – to a much smaller degree – the orthogonal axis (the horizontal axis; notice the highly different scaling of the axes).

This behaviour results from the sequential performance of two rotations (around two axes) of the reflector cube, i.e., it is connected to the specific mechanical coupling of the two stacked rotational axes of the tilting unit. To account for the possible influences of this minimal (5%) engagement of the secondary axis of the affected reference autocollimator on its angle measurement, it needs to be calibrated more extensively. This can be achieved, e.g., by performing several calibrations of the autocollimator's main axis along parallel lines at different angle values of its secondary axis and by repeating the calibrations of the utilised angular field at different rotational angles of the autocollimator around its optical axis with respect to the primary angle standard WMT 220.

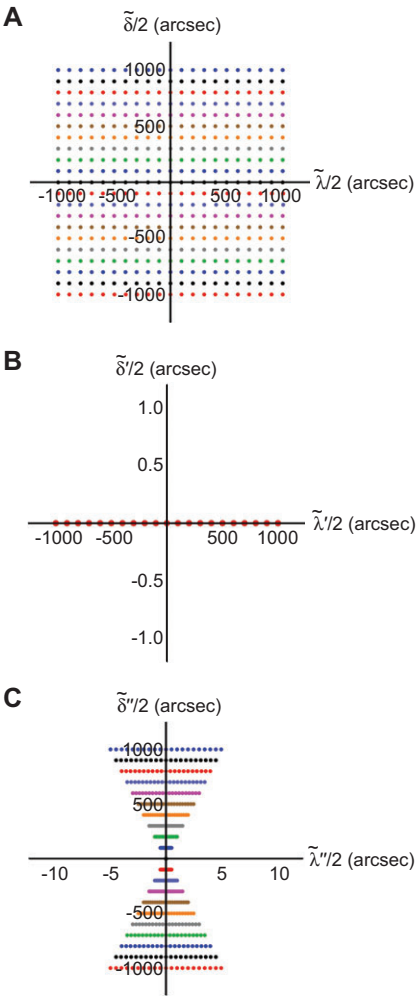

Figure 6 Polar coordinates of the deflected autocollimator beams in the SAAC setup (as detected locally by each autocollimator) when the reflector cube scans a regular grid of spatial angles for the autocollimator to be calibrated. Angles have been divided by a factor of 2 so that they correspond to the angles measured by the autocollimator to be calibrated (A), the horizontal reference autocollimator (B), and the vertical reference autocollimator (C). Note the different scaling of the axes in the case of (C).

6 Alignment and error compensation strategies

Careful alignment of the optomechanical components is essential for achieving minimal errors in the spatial angle measurement with our SAAC. This topic has proven to be of crucial importance to the performance of deflectometric profilometers, too. In the profilometers, movable pentaprisms or optical squares are used for deflecting the autocollimator beam by 90° towards the surface under test and for scanning the surface. This deflection angle is highly stable in the presence of angular errors in the orientation of the prism due to its mechanical shifting by a linear stage. A reduction of the influence of the angular errors (due to the shifting of the pentaprism) on the angle measurement with the autocollimator by a factor of at least 1000 is achievable, however, only if all the components of the deflectometric setup have been properly aligned. In [30], we provided an in-depth analysis of profilometer alignment (and of the pentaprism's optical properties) and derived easy-to-use procedures for the *in situ* alignment of the pentaprism/optical square and the surface under test relative to the autocollimator's measuring axes and its optical axis, which make use of the autocollimator's angle readings only.

In the deflectometric profilometers, optical squares, which consist of two reflecting surfaces, are preferred over solid pentaprisms, which are made out of bulk glass, as the measuring beam is not affected by, e.g., the inhomogeneities in the glass. The reflective surfaces of the optical square need to be aligned with respect to each other. Together with Advanced Light Source (ALS), Berkeley, USA, and the Helmholtz-Zentrum Berlin (HZB), Germany, we developed *in situ* alignment procedures, which provide a definitive solution to this problem and the alignment of deflectometric profilometers with optical squares, in general [31, 32].

In the case of our SAAC, even after careful manufacturing and alignment during assembly, a number of errors will affect its operation, e.g., the remaining alignment errors of its optomechanical components (autocollimators, reflector cube, two-axis tilting stage), the non-orthogonality of the surfaces of the reflector cube, the non-orthogonality of the rotational axes of the tilting unit and the non-orthogonalities of each autocollimator's measuring axes and its optical axis. Some errors, such as the relative angular orientations of the cube's faces, can be characterised in advance by means of our primary angle standard WMT 220. The remaining ones, however, need to be characterised *in situ* by appropriate calibration procedures.

To this end, we derived complete analytical derivations of the angle measurements by the measuring axes of the autocollimators in the SAAC setup in the presence of all alignment errors. For the brevity of this paper, we are not providing them. This model will be used to analyse SAAC data from a suitable set of calibration measurements, e.g., by scanning a regular grid of angles of the reflector cube in pitch and yaw as shown in Figure 6, to retrieve all relevant alignment errors by an optimisation algorithm, which fits the model to the data. Afterwards, the alignment parameter set from the calibration run can be used during the operation of the SAAC for an online

correction of the error influences, which allows deriving the true spatial angular orientation of the reflector cube from the angle measurements by the SAAC's reference autocollimators with lowest uncertainty. In addition, autocollimator calibrations with the SAAC, in which the autocollimator is rotated around its optical axis, allow evaluating the limits of the *in situ* calibration procedure. This approach of utilising redundant data to derive errors also includes advanced error-separating shearing techniques for the cross-calibration of angle measuring devices (see Section 2 for details).

Note that in the derivations in Section 5, we have neglected parasitic rotations of the reflector cube around the x axis (roll angle) due to, e.g., the non-orthogonality of the rotational axes of the tilting unit. This and other effects have been fully included in our extended model. The angle measurements of the cube's faces by the SAAC's reference autocollimators allow evaluating the cube's spatial angular orientation completely. The measuring axes of the horizontal reference autocollimator are sensitive to the cube's rotations with respect to the x and z axes of the coordinate system in Figure 3 (roll and yaw angles), whereas the vertical reference autocollimator's axes are sensitive to x and y rotations (roll and pitch angles). The autocollimator to be calibrated is sensitive to the cube's rotations with respect to the y and z axes (pitch and yaw angles).

7 Description of the SAAC setup

Figures 7 and 8 show the centrepiece of the SAAC, the precision two-axis tilting unit, which has been custom built to PTB's demanding specifications by the Q-Sys BV Company, Helmond, Netherlands. It rotates the reflector cube around two orthogonal axes (the z axis and, due to the specific mechanical stacking of the axes, the corotated y axis in Figure 3; the angles correspond to the rotation angles λ and δ in Figure 4) within an angular range of ±2000 arcsec. The repeatability of the cube's positioning has been specified as ±0.02 arcsec, which is sufficient for the sampling angle deviations of autocollimators densely enough to resolve the deviations on the angular scales, which correspond to the pixel sizes of the typical autocollimator CCDs (see Figure 2). Precise and fast positioning is required; therefore, angular positioning needs to be finished within 1 s, including settling time.

For both rotational axes, the same air-bearing spindles are utilised (see Figure 7). They were manufactured by Professional Instruments Company, Hopkins, MN, USA, and

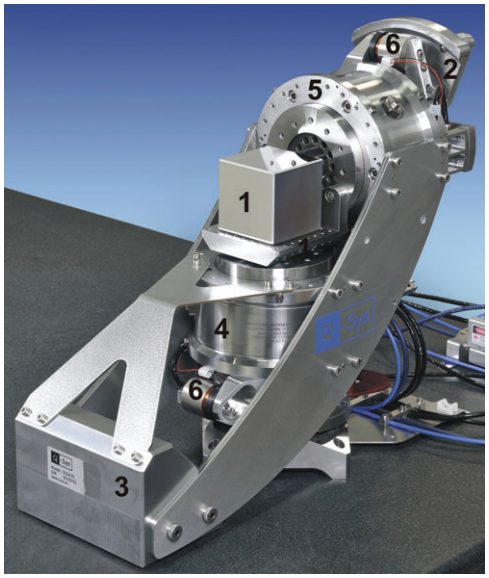

Figure 7 The centrepiece of the SAAC, the precision two-axis tilting unit for rotating the reflector cube (1) around two orthogonal axes. The centre of the rotation is located at the centre of the cube, which is important for minimising error influences. Counterweights (2, 3) locate the centre of the mass close to this point, too, for achieving a well-balanced design. The stacking of two air-bearing rotational axes (4, 5) is apparent. Two of four voice coil actuators (two per axis) are visible (6).

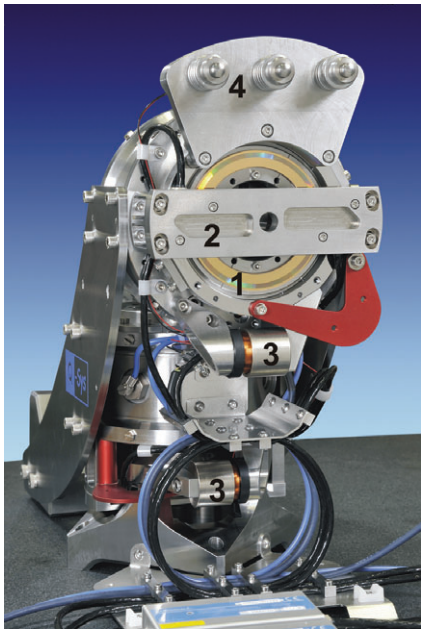

Figure 8 Backside view of the two-axis tilting unit. The circular angle encoder (1) of one of the stacked rotational axes is exposed. Each encoder is read out by a pair of diametrically opposed reading heads, which are hidden behind a supporting bar (2). Two of four voice coils (two per axis) are visible (3), which drive the rotations of the axes and which are placed symmetrically pairwise with respect to each rotational axis to minimise parasitic forces (their counterparts are hidden).

provide excellent positional stability with a radial stiffness of 60 N/µm, axial stiffness of 175 N/µm and tilting stiffness of 0.225 Nm/µrad. The nonreproducible nutation is below 0.01 µrad, and the concentricity deviation does not exceed 25 nm for a full rotation of the bearing. Stop collars restrict the movement range of each axis to 6000 arcsec pv; they are also used for the initialisation of the system. Owing to the specific stacking of two rotational axes, which are connected at their contact point by a flexure hinge for improved stability, the centre of rotation is placed at the centre of the reflector cube. This is important for minimising error influences due to the lateral shifting of the cube's reflecting surfaces with respect to the autocollimator beams when the cube is rotated.

Two voice-coil actuators combined with two measurement systems are applied per axis for the angular positioning of the reflector cube. The voice-coil actuators by Moticont, Van Nuys, CA, USA, are regulated by the control system at a frequency of 100 Hz. The pairs of sensing heads and actuators used for each axis are attached diametrically opposed to compensate for the eccentricities of the axes and to minimise nonradial moments. Owing to the well-balanced design with respect to each rotational axis, which is achieved by several counterweights, the power dissipation is below 135 mW per actuator for the requested positioning time scale. Integrated encoders are used for closed-loop control of the positioning. Sony BH20 (Magnescale, Kanagawa, Japan) sensing heads read out a radial grating (82 mm in diameter) with a graduation period of 250 nm, achieving a resolution of 6 µrad (per head). An interpolation with a factor of 1000 is performed by the Magnescale BD96 interpolation electronics with an *in situ* correction of the interpolation errors (with a remaining typical interpolation error of approximately 5 nrad). The connection between the sensors and actuators is established by a UMAC system of Delta Tau Ltd, Clacton-on-Sea, UK. The UMAC system will be linked to a laboratory PC, from which the calibration procedures are controlled.

Two reflector cubes with different reflectivities of the cube's optical surfaces were manufactured by Carl Zeiss Jena GmbH, Jena, Germany. High demands are placed on the optical and geometrical qualities of the reflector cubes due to the small lateral shifts of each cube's optical surfaces with respect to the autocollimator beams, when it is rotated around its centre, and due to achieving a precise Cartesian arrangement of the autocollimators in our SAAC setup. The cubes are made of quartz, which provides a better long-term stability compared to materials like Zerodur. Their dimensions are 65×65×65 mm^3. For a strainless mounting, quartz cylinders were attached to the bottom surfaces. One cube features a special aluminium coating, which provides a reflectivity of >90% for wavelengths of 400–700 nm, while the second cube was left uncoated for a low reflectivity (approximately 4%). In this way, consistent calibration conditions to accommodate various surfaces under test in optics and synchrotron metrology can be provided. The deviations from orthogonality of the optically utilised surface areas with respect to each other are <1.17 arcsec, which is important to our Cartesian autocollimator arrangement with the SAAC setup. The measured planarity of these surfaces is better than λ/50 pv (or 13 nm pv at λ=633 nm).

Figure 9 shows the final design of the complete SAAC calibration setup, which will be finished at the end of 2012. It integrates all components (two-axis tilting unit plus reflector cube, horizontal and vertical reference autocollimators, the autocollimator to be calibrated) to realise the Cartesian arrangement described in Sections 4 and 5. It will be installed in PTB's clean-room facility and, thus, will operate under favourable environmental conditions, such as a highly stable ambient temperature (ΔT<0.05 K), a constant laminar air flow (v=20 cm/s) and vibration isolation (by mounting the system on a concrete basement, which is separated from the walkable floor and, additionally, by means of passive vibration dampening). As most deflectometric profilometers use a movable pentaprism to scan the surface under test, which induces large changes in the optical path length of the autocollimator beam in the range of 1–2 m, the capability for an automatic adjustment of the path length between the autocollimator and the reflector cube has been implemented in the design.

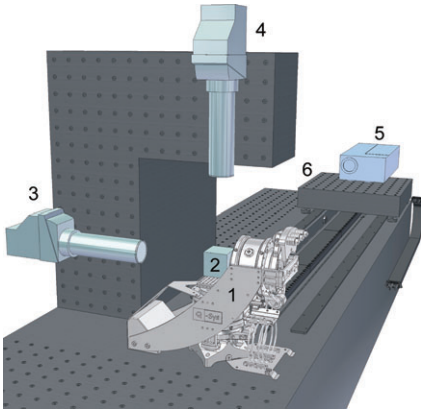

Figure 9 Final design of the complete SAAC setup. Its key component is the precision two-axis tilting unit (1); it rotates the reflector cube (2), which all autocollimators are facing in a Cartesian arrangement. The two reference autocollimators, a horizontal (3) and a vertical (4) one, are mounted on a granite bridge. The autocollimator to be calibrated (5) is located on a linear stage (6) for the automatic adjustment of different beam path lengths, i.e., distances between the autocollimator and the reflector cube.

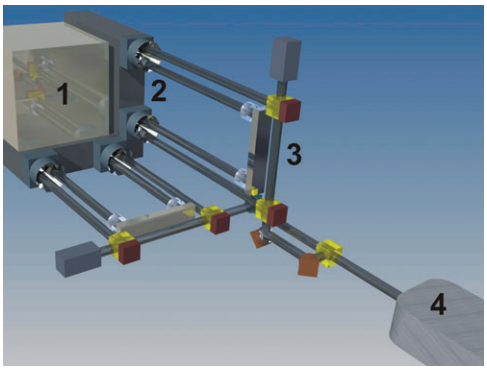

Figure 10 Concept of a two-axis angle interferometer for the additional measurement of the relative angular orientation of the SAAC's movable linear stage with respect to the reflector cube (1) to enable dynamic changes in the autocollimator's distance from the cube. For the measurement of the horizontal and vertical angles, an L-shaped assembly of retroreflectors (2) is mounted to the cube, and a similar assembly of beam splitters, plane mirrors and phase plates (3) is mounted to the movable linear stage, which shifts the autocollimator. The laser (4) is located in the lower right corner in the picture.

To this end, the autocollimator to be calibrated is placed on a linear stage (travel range 1.5 m) with a 500×500 mm^2 movable table top. Initially, calibrations will be performed at discrete distances between the autocollimator and the reflector cube. However, in the near future, we plan to incorporate a two-axis angle interferometer for the measurement of the relative angular orientation of the SAAC's movable linear stage (and the comoving autocollimator on it) with respect to the reflector cube to enable dynamic changes in the autocollimator's distance from the cube (see Figure 10).

8 Conclusions

The form measurement of optics for synchrotron beamlines and FEL has been greatly advanced by the development of highly accurate, autocollimator-based surface profilometers. The size (up to 1.5 m) and extremely stringent shape tolerances (2 nm pv in form, 50 nrad rms in slope) of the beam-shaping optical surfaces for EUV- and X-ray light sources have led to equally stringent demands on the characterisation and traceable calibration of autocollimators, which far surpasses the demands of industrial autocollimator applications in precision engineering. In the case of deflectometric profilometers, the limits of the angle measurement with the autocollimator define the limits of the form measurement. Ultimately, these limits define the manufacturing limits of beam-shaping optics by advanced surface modification technologies. In recent years, great progress has been made at PTB and at synchrotron metrology laboratories in this field. However, important challenges remain, such as the extension of traceable angle calibration from the plane to spatial angles, which require innovative strategies and novel equipment for advanced autocollimator characterisation and calibration with lowest uncertainties. In this contribution, we presented our efforts at PTB to develop and set up a novel system, which makes use of an innovative Cartesian arrangement of three autocollimators and which provides traceability of spatial angle measurement to a conventional plane angle standard.

9 Author contributions

Concerning this joint research paper, all authors have contributed equally to the formulation of the scientific questions, measurement of experimental data, realisation of the presented device, and the formulation of this manuscript. Submission of this paper has been approved by PTB's Presidential Board and all authors have signed documents stating that PTB's QM-VA 16 'Rules for Ensuring Good Scientific Practice' have been complied with.

Acknowledgements: The authors would like to thank Valeriy V. Yashchuk of ALS, Lawrence Berkeley National Laboratory, Berkeley, USA, and Frank Siewert and Thomas Zeschke from BESSY II, Helmholtz-Zentrum Berlin, Germany, for the productive research collaboration on autocollimator-based profilometers.

Part of this research was funded by the EMRP project IND10 (**http://www.ptb.de/emrp/ind10-home.html**). We thank the EMRP for the financial support of this work. The EMRP is jointly funded by the EMRP participating countries within EURAMET and the European Union.

Received September 6, 2012; accepted September 25, 2012

Appendix

If a measurement beam from an autocollimator with a normalised direction vector $\hat{u}$ is reflected at the surface of a reflector with normal vector $\hat{n}$, the normalised direction vector $\hat{u}_r$ of the reflected beam is obtained as

$$\hat{u}_r = \hat{u} - 2\langle \hat{u}\hat{n}\rangle \cdot \hat{n}, \tag{A1}$$

with $\langle \hat{u}\hat{n}\rangle$ symbolizing the vector product and $|\hat{n}|=|\hat{u}|=|\hat{u}_r|=1$.

In the x-y-z coordinate system from Figure 4, the normal vector $\hat{n}$ of the cube's reflecting frontal surface is given by

$$\hat{n} = \begin{pmatrix} \cos\lambda\cos\delta \\ \sin\lambda\cos\delta \\ \sin\delta \end{pmatrix}. \tag{A2}$$

For the autocollimator to be calibrated, let its measuring beam be incident in the direction of the negative x axis, i.e.,

$$\hat{u} = \begin{pmatrix} -1 \\ 0 \\ 0 \end{pmatrix}. \tag{A3}$$

The vector of the reflected beam $\hat{u}_r$ then results from (A1) and (A2) as

$$\hat{u}_r = \begin{pmatrix} 2\cos^2\lambda\cos^2\delta - 1 \\ \sin(2\lambda)\cos^2\delta \\ \cos\lambda\sin(2\delta) \end{pmatrix}. \tag{A4}$$

The polar coordinates $\tilde{\lambda}$ and $\tilde{\delta}$ of the reflected beam can be defined from (A2) and (A4) via

$$\begin{pmatrix} \cos\tilde{\lambda}\cos\tilde{\delta} \\ \sin\tilde{\lambda}\cos\tilde{\delta} \\ \sin\tilde{\delta} \end{pmatrix} = \begin{pmatrix} 2\cos^2\lambda\cos^2\delta - 1 \\ \sin(2\lambda)\cos^2\delta \\ \cos\lambda\sin(2\delta) \end{pmatrix} \tag{A5}$$

so that by comparing the components of (A5), we obtain

$$\sin\tilde{\delta} = \cos\lambda\sin(2\delta) \quad \text{and} \tag{A6}$$

$$\sin\tilde{\lambda} = \frac{\sin(2\lambda)\cos^2\delta}{\sqrt{1-\cos^2\lambda\sin^2(2\delta)}}. \tag{A7}$$

In the case of the horizontal reference autocollimator, its optical axis and its horizontal and vertical measuring axes correspond to the y, (-x) and z axes, respectively (see Figure 4). In the x-y-z coordinate system, the normal vector $\hat{n}'$ of the cube's surface, which faces the horizontal reference autocollimator, is given by

$$\hat{n}' = \begin{pmatrix} -\sin\lambda \\ \cos\lambda \\ 0 \end{pmatrix}, \tag{A8}$$

and its measuring beam is incident in direction of the negative y axis. With this and (A8), the vector of the reflected beam $\hat{u}_r'$ results from (A1) as

$$\hat{u}_r' = \begin{pmatrix} -\sin(2\lambda) \\ \cos(2\lambda) \\ 0 \end{pmatrix}. \tag{A9}$$

For a better intuitive understanding of the results, we define a new polar coordinate system with angles $\tilde{\lambda}'$ and $\tilde{\delta}'$, which are connected to the horizontal reference autocollimator, i.e., the new polar coordinates represent a local view of the beam deflection by this autocollimator. The x-y-z coordinates are then replaced by the y-(-x)-z coordinates. Therefore, the polar coordinates $\tilde{\lambda}'$ and $\tilde{\delta}'$, of the reflected beam can be defined from (A2) and (A9) via

$$\begin{pmatrix} \cos\tilde{\lambda}'\cos\tilde{\delta}' \\ \sin\tilde{\lambda}'\cos\tilde{\delta}' \\ \sin\tilde{\delta}' \end{pmatrix} = \begin{pmatrix} \cos(2\lambda) \\ \sin(2\lambda) \\ 0 \end{pmatrix}. \tag{A10}$$

By comparing the components of (A10). We obtain

$$\tilde{\delta}' \equiv 0 \quad \text{and} \tag{A11}$$

$$\tilde{\lambda}' = 2\lambda. \tag{A12}$$

In the case of the vertical reference autocollimator, its optical axis and its horizontal and vertical measuring axes correspond to the z, y and (-x) axes, respectively (see Figure 4). In the x-y-z coordinate system, the normal vector $\hat{n}''$ of the cube's surface, which faces the vertical reference autocollimator is given by

$$\hat{n}'' = \begin{pmatrix} -\cos\lambda\sin\delta \\ -\sin\lambda\sin\delta \\ \cos\delta \end{pmatrix}, \tag{A13}$$

and its measuring beam is incident in direction of the negative z axis. With this and (A13), the vector of the reflected beam $\hat{u}_r''$ results from (A1) as

$$\hat{u}_r''=\begin{pmatrix}-\cos\lambda\sin(2\delta)\\-\sin\lambda\sin(2\delta)\\\cos(2\delta)\end{pmatrix}. \tag{A14}$$

We again define a new polar coordinate system with angles $\tilde{\lambda}''$ and $\tilde{\delta}''$, which represent a local view of the beam deflection by the vertical reference autocollimator. The x-y-z coordinates are then replaced by the z-y-(-x) coordinates. Therefore, the polar coordinates $\tilde{\lambda}''$ and $\tilde{\delta}''$ of the reflected beam can be defined from (A2) and (A14) via

$$\begin{pmatrix}\cos\tilde{\lambda}''\cos\tilde{\delta}''\\\sin\tilde{\lambda}''\cos\tilde{\delta}''\\\sin\tilde{\delta}''\end{pmatrix}=\begin{pmatrix}-\cos\lambda\sin(2\delta)\\-\sin\lambda\sin(2\delta)\\\cos(2\delta)\end{pmatrix}. \tag{A15}$$

By comparing the components of (A15), we obtain

$$\sin\tilde{\delta}''=\sin\tilde{\delta}=\cos\lambda\sin(2\delta) \quad \text{and} \tag{A16}$$

$$\sin\tilde{\lambda}=\frac{-\sin\lambda\sin(2\delta)}{\sqrt{1-\cos^2\lambda\sin^2(2\delta)}}. \tag{A17}$$

References

[1] F. Siewert, J. Buchheim, S. Boutet, G. J. Williams, P. A. Montanez, et al., Opt. Express 20, 4525–4536 (2012).

[2] G. Ehret, M. Schulz, M. Stavridis and C. Elster, Meas. Sci. Technol. 23(094007), 1–8 (2012).

[3] F. Siewert, J. Buchheim, T. Zeschke, G. Brenner, S. Kapitzki, et al., Nucl. Instrum. Methods Phys. Res., Sect. A 635, 52–57 (2011).

[4] Z. Ali, N. A. Artemiev, C. L. Cummings, E. E. Domning, N. Kelez, et al., Proc. SPIE Int. Soc. Opt. Eng. 8141(81410O), 1–15 (2011).

[5] V. V. Yashchuk, S. Barber, E. E. Domning, J. L. Kirschman, G. Y. Morrison, et al., Nucl. Instrum. Methods Phys. Res., Sect. A 616, 212–223 (2010).

[6] M. Schulz, G. Ehret and A. Fitzenreiter, J. Eur. Opt. Soc. Rapid Publications 5(10026), 1–4 (2010).

[7] J. L. Kirschman, E. E. Domning, W. R. McKinney, G. Y. Morrison, B. V. Smith, et al., 'Proc. SPIE Int. Soc. Opt. Eng. 7077(70770A), 1–12 (2008).

[8] H. Sinn, J. Gaudin, L. Samoylova, A. Trapp and G. Galasso, 'X-Ray Optics and Beam Transport', (European X-Ray Free-Electron Laser Facility GmbH, Hamburg, Germany, 2011), http://edmsdirect.desy.de/edmsdirect/file.jsp?edmsid=2081421 (last accessed 2012-08-03).

[9] L. Samoylova, H. Sinn, F. Siewert, H. Mimura, K. Yamauchi, et al., Proc. SPIE Int. Soc. Opt. Eng. 7360, 1–9 (2009).

[10] R. D. Geckeler, A. Just, M. Krause and V. V. Yashchuk, Nucl. Instrum. Methods Phys. Res., Sect. A 616, 140–146 (2010).

[11] R. D. Geckeler and A. Just, Proc. SPIE Int. Soc. Opt. Eng. 7077(70770B), 1–12 (2008).

[12] R.D. Geckeler and A. Just, Proc. SPIE Int. Soc. Opt. Eng. 6704(670407), 1–12 (2007).

[13] R. Probst, R. Wittekopf, M. Krause, H. Dangschat and A. Ernst, Meas. Sci. Technol. 9, 1059–1066 (1998).

[14] W. T. Estler, J. Res. Natl. Inst. Stand. Technol. 103, 141–151 (1998).

[15] P. J. Sim, Angle standards and their calibration in 'Modern Techniques in Metrology', Ed. by P. L. Hewitt (World Scientific, Singapore, 1984), pp. 102–121.

[16] E. Debler, Zeitschrift für Vermessungswesen 102, 117–126 (1977).

[17] C.P. Reeve, 'The calibration of indexing tables by subdivision', NBS Internal Report, 75-750 (NIST, Gaithersburg, US, 1975).

[18] R. D. Geckeler, A. Fricke and C. Elster, Meas. Sci. Technol. 17, 2811–2818 (2006).

[19] R. Probst, Meas. Sci. Technol. 19(015101), 1–11 (2008).

[20] A. Just, M. Krause, R. Probst, H. Bosse, H. Haunerdinger, et al., Precis. Eng. 33, 530–533 (2009).

[21] A. Just, M. Krause, R. Probst and R. Wittekopf, Metrologia 40, 288–294 (2003).

[22] V. V. Yashchuk, W.R. McKinney, T. Warwick, T. Noll, F. Siewert, et al., Proc. SPIE Int. Soc. Opt. Eng. 6704(67040A), 1–12 (2007).

[23] C. Elster, Appl. Opt. 39, 5353–5359 (2000).

[24] C. Elster, J. Comput. Appl. Math. 110, 177–180 (1999).

[25] C. Elster and I. Weingärtner, Appl. Opt. 38, 5024–5031 (1999).

[26] 'International Vocabulary of Metrology – Basic and General Concepts and Associated Terms', JCGM 200:2012, http://www.bipm.org/en/publications/guides/vim.html (last accessed 2012-08-01).

[27] 'Evaluation of measurement data – Guide to the expression of uncertainty in measurement', JCGM 100:2008, http://www.bipm.org/en/publications/guides/gum.html (last accessed 2012-08-01).

[28] http://www.bipm.org/en/si/ (last accessed 2012-08-01).

[29] R. Probst, G. Fütterer, J. Illemann, J. Mokros, P. K. Lui, et al., Proc. 7th Int. Conf. European Society for Precision Engineering and Nanotechnology 2, 121–124 (2007).

[30] R. D. Geckeler, Meas. Sci. Technol. 18, 115–125 (2007).

[31] S. K. Barber, R. D. Geckeler, V. V. Yashchuk, M. V. Gubarev, J. Buchheim, et al., Opt. Eng. 50(073602), 1–8 (2011).

[32] S. K. Barber, G. Y. Morrison, V. V. Yashchuk, M. V. Gubarev, R. D. Geckeler, et al., Opt. Eng. 50(053601), 1–10 (2011).

Ralf D. Geckeler received his PhD from the Eberhard-Karls University, Tübingen, Germany, in 1998. He heads the Angle Metrology Group at PTB, Braunschweig, the National Metrology Institute of Germany. The group focuses on research and development, as well as the calibration of angle-measuring devices, such as autocollimators and angle encoders, in international collaboration with industry and research institutes. Current research topics include the improvement of autocollimator performance and calibration, especially at small beam diameters, the advancement of angle metrology for the characterisation of beamline optics at synchrotron and FEL facilities worldwide, and the development of methods and advanced mathematical algorithms for angle encoder calibration. The group is currently the pilot laboratory for the international EURAMET.L-K3.2009 Key Comparison on autocollimator calibration with 27 participating NMI.

Oliver Kranz received his degree in physics from the Leibniz Universität, Hannover, Germany, in 2009. He works as a PhD student in the Angle Metrology Group at PTB, Braunschweig. His work focuses on the characterisation of autocollimators in experiments, ray-tracing simulations and mathematical modelling. In addition, he is involved in the development of a 2D calibration system for autocollimators.

Andreas Just received his degree from the Technical University 'Otto von Guericke', Magdeburg, Germany, in 1986. He is a member of the Angle Metrology Group at PTB, Braunschweig. His work focuses on the calibration of angle standards and instruments, such as autocollimators, and the development of new calibration methods.

Michael Krause received his degree from the University of Applied Sciences, Lübeck, Germany, in 1987. He is a member of the Angle Metrology Group at PTB, Braunschweig. His work focuses on angle-encoder calibrations and the development of software for the analyses of self- and cross-calibration data from these encoders, including PTB's primary angle standard WMT 220 for the SI unit 'radian'. He is also responsible for the automatisation of calibration setups.